Developmental Biology 403 (2015) 89–100

Contents lists available at ScienceDirect

Developmental Biology

journal homepage: www.elsevier.com/locate/developmentalbiology

PIAS-like protein Zimp7 is required for the restriction of the zebrafish organizer and mesoderm development

Roberto Moreno-Ayala, Denhí Schnabel, Enrique Salas-Vidal, Hilda Lomelí *

Departamento de Genética del Desarrollo y Fisiología Molecular Instituto de Biotecnología, Universidad Nacional Autónoma de México, Mexico

ARTICLE INFO

Article history:
Received 6 November 2014
Received in revised form
30 March 2015
Accepted 3 April 2015
Available online 24 April 2015

Keywords:
Zimp7
Zebrafish
Dorsal organizer
Mesoderm development

ABSTRACT

The Zmiz2 (Zimp7) protein and its homolog Zmiz1 (Zimp10) were initially identified in humans as androgen receptor co-activators. Sequence analysis revealed the presence of an SP-RING/Miz domain, which is highly conserved in members of the PIAS family and confers SUMO-conjugating activity. Zimp7 has been shown to interact with components of the Wnt/β-Catenin signaling pathway and with Brg1 and BAF57, components of the ATP-dependent mammalian SWI/SNF-like BAF chromatin-remodeling complexes.

In this work, we analyze the role of zygotic Zimp7 in zebrafish development. We describe evidence indicating that Zimp7 is required for mesoderm development and dorsoventral patterning. Morpholino-mediated reduction of zygotic Zimp7 produced axial mesodermal defects that were preceded by up-regulation of organizer genes such as *bozozok, goosecoid* and *floating head* at the onset of gastrulation and by down-regulation of the ventral markers *vox, vent* and *eve1* indicating loss of the ventrolateral mesoderm. Consistently, embryos overexpressing *zimp7* RNA exhibited midline defects such as loss of forebrain and cyclopia accompanied by transcriptional changes directly opposite of those found in the morphants. In addition, the patterning of ventralized embryos produced by the overexpression of *vox* and *vent* was restored by a reduction of Zimp7 activity. Altogether, our findings indicate that Zimp7 is involved in transcriptional regulation of factors that are essential for patterning in the dorsoventral axis.

Introduction

One of the earliest events occurring during vertebrate embryonic development is the patterning of the embryo into the ectoderm, mesoderm, and endoderm germ layers. In zebrafish, mesoderm derives from the marginal region of the late blastula. Two mesodermal domains are initially induced by the activities of maternal β-Catenin and the Nodal pathway. One of these domains, the dorsal organizer, determines the future dorsal side of the embryo. The cells of the dorsal organizer contribute to axial structures such as the prechordal plate and notochord (Langdon et al., 2011; Schier and Talbot, 2001, 2005). During gastrulation, the dorsal organizer acts as a regulator of dorsoventral axis patterning. The remainder of the mesoderm constitutes the non-axial mesodermal domain. Further patterning of the non-axial mesoderm along the margin from lateral to ventral gives rise to muscle, kidney and blood (Ramel et al., 2005).

Downstream of mesodermal induction, the Vent family homeobox genes *vox, vent* and *ved* function as transcriptional repressors to antagonize axial identity acquisition within non-axial domains (Imai et al., 2001; Gilardelli et al., 2004; Shimizu et al., 2002). These repressors prevent the transcription of dorsal organizer genes such as *goosecoid (gsc)* (Schultemerker et al., 1994; Toyama et al., 1995) and *chordin (chd)* (Miller-Bertoglio et al., 1997), which in turn prevent ventral gene expression (Ramel and Lekven, 2004; Kawahara et al., 2000). A critical factor for the regulation of the Vent homeodomain family is the secreted ligand Wnt8a. Wnt8a (Lekven et al., 2001; Hikasa and Sokol, 2013; Baker et al., 2010) signaling plays additional roles during mesodermal development. During gastrulation, Wnt8a signaling regulates the expression of several mesodermal ventrolateral markers required for the maintenance and proliferation of non-axial mesoderm (Baker et al., 2010; Ramel et al., 2005). In addition, Wnt signaling originating in the lateral mesodermal precursors acts on anterior neuroectoderm to posteriorize the neural tissue (Erter et al., 2001). In the absence of Wnt8a, embryos present expansion of axial mesoderm at the expense of ventrolateral mesoderm and expansion of the neuroectoderm (Baker et al., 2010). At 24 h post-fertilization (hpf), Wnt8a mutants display dorsalized phenotypes that are characterized by axial defects and the absence of trunk and tail structures (Lekven et al., 2001). Embryos with increased Wnt signaling exhibit a loss of the forebrain and eyes (Lekven et al., 2001).

One of the earliest genes required for the formation of the dorsal organizer is the homeodomain transcriptional repressor *bozozok (boz)*, which mediates the repression of ventralizing genes such as *vox/vent/ved, bmp2b*, and *wnt8a* (Solnica-Krezel and Driever, 2001).

* Corresponding author.
E-mail address: hilda@ibt.unam.mx (H. Lomelí).

http://dx.doi.org/10.1016/j.ydbio.2015.04.013
0012-1606/

In the absence of *boz*, the shield fails to form and organizer function is unpaired. In addition to *boz*, the TGF-β Nodal signaling pathway is activated by *ndr1/squint (sqt)*, another gene with a key function in patterning the dorsal organizer (Schier, 2009). Mutations in *sqt* and *boz* display axial midline structural defects that are derived from the organizer, including the notochord and prechordal plate (Schier and Talbot, 2001; Feldman et al., 1998; Sampath et al., 1998). Additionally, *sqt* mutants have reduced expression of dorsal mesoderm genes in the late blastula, a failure in shield formation at the onset of gastrulation and at later stages, forebrain defects and cyclopia (Heisenberg and Nusslein-Volhard, 1997). In a similar fashion, *boz* mutants have strongly reduced *gsc* expression and defects in the neural tube (Sirotkin et al., 2000).

Human ZIMP7 protein and its homolog ZIMP10 were initially identified as androgen receptor (AR) co-activators (Sharma et al., 2003). Analysis of their sequence identified the presence of a SP-RING/Miz domain, which is highly conserved in members of the PIAS family (Sharma et al., 2003; Gutierrez et al., 2003). PIAS proteins are involved in the sumoylation process where they act as SUMO-E3-ligases, an activity that is conferred by the SP-RING/Miz domain (Rytinki et al., 2009). The ZIMP proteins share a similarity beyond the SP-RING Zn-finger that is known as the X-SPRING (eXtended SP-RING) domain. This extended similarity is conserved in proteins of several metazoans and defines an independent subfamily (Rodriguez-Magadan et al., 2008).

In addition to their capacity to interact with the AR, the ZIMP proteins have been shown to interact with other hormone nuclear receptors and transcription factors such as p53 and Smad3/Smad4. In most of these cases, the interaction leads to stimulation of transcriptional activity (Lee et al., 2007; Li et al., 2006). Recently, it has been shown that Zimp7 has a role in regulating the activity of the Wnt/β-Catenin signaling pathway in mammalian cells. Zimp7 is shown to physically interact with β-Catenin and enhance Wnt/β-Catenin-mediated transcription (Lee et al., 2013). Moreover, in this report Zmiz2 null mice exhibit down-regulation of Axin2, a downstream target gene of β-Catenin. Intriguingly, null embryos do not present any significant developmental defects.

ZIMP7 and ZIMP10 contain a strong transactivation domain within the C terminus, which they could use directly to function as transcriptional co-regulators (Huang et al., 2005; Sharma et al., 2003). Additionally, the ZIMP proteins interact with BRG1, the catalytic subunit of the SWI-SNF remodeling complex. It has been demonstrated that ZIMP7 increases the effects of BRG1 on androgen receptor-mediated transcriptional activity (Huang et al., 2005). These observations suggest that the ZIMP proteins may be regulating transcription of specific target genes by altering their chromatin structure.

In this study, we analyze the role of zygotic Zimp7 in zebrafish development. For this purpose we used both loss- and gain-of-function strategies. We find that disruption of zygotic Zimp7 with a morpholino and exogenous expression by mRNA injection lead to opposing axial defects. Whereas loss-of-function results in an excessive notochord and floor plate production, expansion of organizer markers and dorsal mesoderm expansion; the gain-of-function results in failure to generate forebrain structures and partial loss of the notochord. Notably, the global morphological defects produced by the morpholinos are recapitulated in CRISPR-Cas induced bi-allelic mutants. We found that expansion of dorsal mesoderm occurs at the expense of the loss of ventrolateral mesodermal fates. With previous results, our findings suggest that Zimp7 could be involved in positive regulation of zygotic Wnt signaling during dorsoventral patterning of zebrafish embryos.

Methods

Fish maintenance

An AB-TU-WIK hybrid line was used and embryos were obtained by natural mating and raised at 28.5 °C based on standard procedures (Westerfield, 2000). Staging was performed according to the Kimmel system (Kimmel et al., 1995).

Morpholino injection

Morpholinos (Gene Tools) were diluted in 1 × Danieau's solution, 4 nl were injected into the yolk cell of 1–2-cell stage embryos. The following amount of morpholino was used: 8 ng of the *zimp7* splicing morpholino (5' AGTCACTGCGGACAGAAACACACTG 3') 24 ng of the *zimp7*-ATG morpholino (5′ CTATGGGACACCCCGAATCTCCTCA 3'), 3 ng of the *foxh1* MO (5′TGCTTTGTCATGCTGATGTAGTGGG3') (Pei et al., 2007), *oep* MO (5' GCCAATAAACTCCAAAACAACTCGA3') (Nasevicius and Ekker, 2000) and *chordin* MO (5' ATCCACAGCAGCCCCTCCATCATCC 3') (Dal-Pra et al., 2006). The standard control morpholino (5' CCTCTTACCTCAGTTACAATTTATA 3') was included in all experiments at the same concentration indicated for the morpholino assayed. To reduce the p53-dependent off-targeting effect at 30 hpf for the evaluation of the *zimp7* morphants phenotype and in rescue experiments, we coinjected the *p53* MO (5' GCGCCATTGCTTTGCAAGAATTG 3') at the same concentration as the morpholino assayed.

To confirm the splicing alterations, the following primers were used 5' ACCCCATCAACTCCATGAAA 3' and 5' CTGGTTCTGCTTCTCCT GTAA 3' and the Amplificasa DNA Polymerase (BioTecMol).

Zimp7 cDNA cloning and mRNA synthesis

Based on the zebrafish Zimp7 gene sequence in Ensembl (ENSDARG00000079812, zmiz2-201 transcript), the first half (1–1663 bp) of the cDNA was amplified using the primers: 5' ATGAACCCCATCAACTCC 3' and 5' CTTCTTCATGAGTCCCTG 3', and then cloned into pCR 2.1 TOPO (Invitrogen). Subsequently, the construction was digested with BamHI and XhoI and inserted into pCS2+. To obtain the second half (1284–2667 bp), the primers 5' ACCCTCGAGTGGTT CTGGAGCCCTTCAGACTGG 3' and 5' AACTCTAGATGGAGGACTGCTGG ACGGTGG3' were used. The PCR product was cloned into pCS2^{+}, double digested with StuI-XbaI and joined with the first half of the zimp7 cDNA. A Kozak sequence was introduced to improve the mRNA translation efficiency with the following primers: 5' AACACTAGTGCCACC**ATG**AACCCCATCAACTCC 3' (Kozak sequence underlined, first codon in bold) and 5' AACCCATGGGTGCTCCGAAAACCTGGCT 3'. The PCR product was digested with SpeI and NcoI and ligated into pCS2^{+}-*zimp7* construction. Before mRNA synthesis, the construction was linearized with NotI. All PCR reactions were performed with Platinum Taq DNA Polymerase High Fidelity (Invitrogen).

For rescue experiments, *boz* (Ro and Dawid, 2009), *sqt* (Feldman et al., 1998), *foxh1/eomesodermin* (Slagle et al., 2011), CA*smad2* (Jia et al., 2008) and *vox/vent* encoding plasmids (kindly provided by Arne Lekven) were used. All mRNA were synthesized with mMessage mMachine kit (Ambion) and diluted in 100 mM KCl; 4 nl were injected in the yolk cell.

In situ hybridization and expression quantification

Whole-mount in situ hybridizations were performed essentially as described previously (Thisse and Thisse, 2008). The probes used were as follows: *eve1* (Joly et al., 1993), *chd* (Miller-Bertoglio et al., 1997), *sox32* (Kikuchi et al., 2001), *wnt8a* (Lekven et al., 2001), *vox/vent* (Melby et al., 2000), *ved* (Shimizu et al., 2002), *flh* (Talbot et al., 1995), *boz* (Ro and Dawid, 2009), *sqt* (Feldman et al., 1998), *lefty1* (Harvey et al., 2010), *shh* (Krauss et al., 1993), *col2a1a* (Yan et al.,

1995), *otx2* (Li et al., 1994), *ntl* (Schultemerker et al., 1992), *hgg1* (Thisse et al., 2001) and *gsc* (Stachel et al., 1993). For the *zimp7* probe, the first half of the complete cDNA (cloned in pCR 2.1 TOPO) was used as template. Embryos were mounted on glicerol and photographed on a Leica MZ 125 microscope equiped with an AxioCam MR5 (Zeiss) camera. For difficult probes (such as *boz* and *sqt*), a buffer containing 2% (w/v) Roche Blocking Reagent (11 096 176 001) was used for blocking instead of BSA and Roche BM Purple alkaline phosphatase substrate (11 442 074 001) as staining solution overnight at R.T.

Estimations of the expression area were performed (except for the ventral genes *vox* and *vent*, for which the marginal expression angle was measured) using ImageJ (NIH) and statistical analysis was done with Prism 5 (GraphPad). The results were normalized to control levels. Two-tailed unpaired *t*-test for normal distribution and Mann–Whitney *U* test for non-parametric distribution were performed.

Real-time PCR analysis

Trizol Reagent (Ambion) was used for RNA extraction with 20 embryos following the manufacturer's instructions. After Dnase I (Thermo) treatment, 500 ng were used for reverse transcription with M-MLV (Invitrogen) with oligo dT. cDNA was diluted 1:40 in 20 µl quintuplicate reactions. The Maxima SYBR Green Reagent (Thermo) was used for qPCR in a Light Cycler 480 (Roche), using the following program: 95 °C, 5 min; (95 °C, 15 s; 58 °C, 20 s; 72 °C, 30 s-single quantification at this step-) × 40 cycles; and a melting curve from 72 to 95 °C holding during 5 s each 0.5 °C was performed. A relative quantification with the Light Cycler 480 software was performed with at least three of the five replicates that displayed similar reaction curves, after normalizing to the expression level of the elongation factor 1 alpha (*ef1alpha*) and using a second derivative maximum method. *ef1alpha, vox,* and *vent* primers were reported in Flores et al. (2008) and *sqt* in Li et al. (2011). The rest were designed with Perl Primer. Sequences are the following:

bozFq 5' GCAACCGTGGCCTTATGCCG 3'
bozRq 5' TCGCTCGAGCTGCTCCGTCT 3'
gscFq 5' CCTTGGTTCGCAACAGTGTC 3'
gscRq 5' GCTGCTCGTCGGTGAAAATG 3'

Zimp7 CRISPR/Cas-mediated mutations and T7 EI assay

The *zimp7* genomic target sequence is 5' GGCATGTACGGCCGG CCCAGCGG 3', located at exon 3. The primers 5' TAGGCATG-TACGGCCGGCCCAG 3' and 5' AAACCTGGGCCGGCCGTACATG 3' were annealed and cloned into the pDR274 plasmid (Hwang et al., 2013); sgRNA was synthesized using T7 RNA polymerase (Roche). The AmpliCap SP6 High Yield Message (CellScript) was used for the Cas9 mRNA synthesis using the pCS2-nls-zCas9-nls plasmid (Jao et al., 2013). Both transcripts were purified using a QIAprep column (QIAGEN). 1-Cell stage embryos were injected directly into the cell with 2 nl of solution containing ~13 ng/µl of sgRNA, ~400 ng/µl of Cas9 mRNA diluted in 100 mM KCl.

The targeted genomic locus was amplified from single embryos using the following primers: 5' CTAATGATTCAGGTGCGTGTTG 3' and 5' TCACCCACTCACACACTCTCTC 3', which anneal ~220 and ~60 bp upstream and downstream from the predicted cut site, respectively, with Phusion High-Fidelity DNA Polymerase (Thermo). The products were purified for T7 EI (NEB) assay and to clone into pJET (Thermo) for sequencing. The PCR products of five embryos which presented an altered phenotype and five randomly chosen embryos with

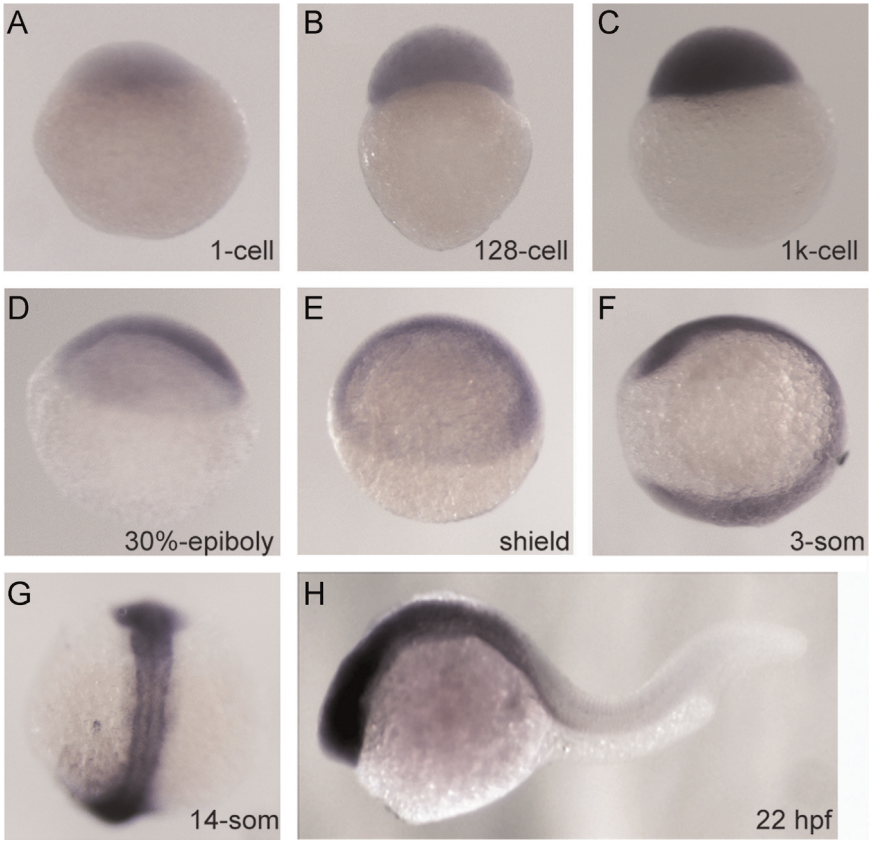

Fig. 1. Spatiotemporal Expression Pattern of *zimp7* Expression pattern of *zimp7* detected by whole-mount in situ hybridization, at indicated stages. (A–E), lateral views with the animal pole oriented at the top; (F), lateral with anterior at the top; (G), dorsal view with anterior at the top (H), anterior is oriented towards the left.

normal appearance were used to perform the T7 EI assay, with a total of ~200 ng, treated for 20 min and resolved in a 2.5% agarose gel.

Results

Spatiotemporal expression of Zimp7

Previously we reported a phylogenetic tree and the structural relationships among X-SPRING subfamily genes of different species including *Danio rerio* (Rodriguez-Magadan et al., 2008). Despite the genome duplication of zebrafish, there is only one *zimp7* gene. Zimp7 protein shares a sequence identity of 71.36% and 71.79% to human and mouse Zimp7, respectively.

We generated a full-length *zimp7* cDNA construct and examined the spatiotemporal expression pattern during zebrafish embryogenesis using whole-mount in situ hybridization (WISH). Maternal *zimp7* transcripts were present at high levels in one-cell embryos and in all blastodermal cells of the early embryo (Fig. 1A and B). After the midblastula transition (MBT), strong zygotic expression of *zimp7* was broadly detected in embryos at all stages analyzed (Fig. 1C–H).

Alterations in Zimp7 levels produce midline defects

To determine the role of Zimp7 in embryogenesis, we used an antisense morpholino (*zimp7*-sp MO) targeted to a splice donor site of the premature *zimp7* mRNA that is expected to prevent splicing. The splicing block results in a frameshift mutation that causes a short truncated peptide to be produced and generates a zygotic loss-of-function situation. The majority of embryos injected with 8 ng of *zimp7*-sp MO at 9–10 hpf, appeared elongated with an ovoid-shaped gastrula as in dorsalization (Fig. 2A and B). Later, at 30 hpf, the embryos exhibited axial defects with ventral body curvature and a kinked notochord (Fig. 2C). Additional defects were observed with less frequency, including reduced or absent trunk or tail structures (Supplementary Fig. S1A). Although

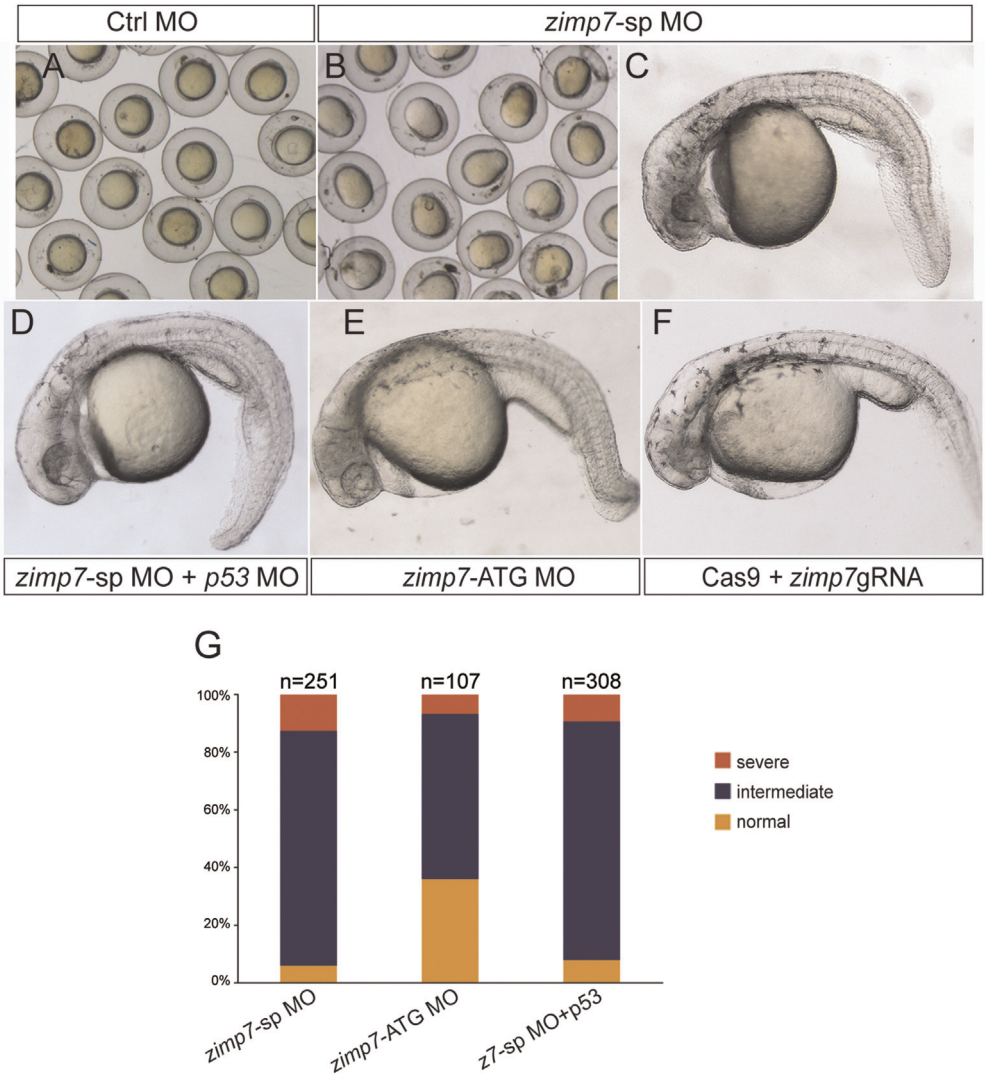

Fig. 2. Zimp7 loss-of-function causes axial phenotypes. (A) Embryos injected with a control MO at 9 hpf; relative to this embryos. (B) *zimp7*-sp MO injected embryos present an elongated shape. (C) After 30 hpf of development, *zimp7*-sp MO injected embryos are ventrally curved. (D) Co-injection of embryos with the *zimp7*-sp MO and the *p53* MO rescued head defects but not axial defects. (E) At 30 hpf embryos injected with a *zimp7*-ATG MO present a similar phenotype. (F) Embryos with specific mutations in the *zimp7* gene produced by the CRISPR/Cas system present a curly down tail and a similar appearance as the *zimp7*-sp MO injected embryos. (G) Distribution of phenotypes produced with the injected morpholinos. Total numbers of embryos are shown at the top.

zimp7 morphants display cell death in head structures, this defect was rescued by the co-injection of the *zimp7*-sp MO with one previously used to reduce p53 activity (*p53* MO), while the axial defects persisted (Fig. 2D and Supplementary Fig. S1B). Altered splicing was confirmed using PCR (Supplementary Fig. 1D). In addition, we injected an ATG-targeted MO designed to block translation, which caused similar embryonic defects at 30 hpf (Fig. 2E). Moreover, rescue experiments supporting MO specificity will be presented later (Fig. 7). Ratios of embryos with the observed morphology as shown are summarized in Fig. 2G.

As a complementary confirmation of the MO-induced phenotype specificity, we induced mutagenesis of the *zimp7* gene with the CRISPR/Cas system (Hwang et al., 2013; Jao et al., 2013). A number of the Cas9/*zimp7*-gRNA injected embryos exhibited similar morphologies at 30 hpf as those ones observed with the injection of MOs (Figs. 2F and S1C). T7 EI analysis and sequence of genomic DNA obtained from embryos with malformations confirmed the presence of specific mutations in the *zimp7* gene (Supplementary Fig. S1E and F), suggesting that the phenotype is produced by bi-allelic mutations. Since transgenic knock-outlines are no yet established we continued our analysis in the *zimp7*-sp MO injected embryos.

To further investigate the role of Zimp7 in embryonic development, we injected zebrafish embryos with synthetic *zimp7* mRNA. Injection of *zimp7* mRNA causes axial mesoderm defects resembling previously described Nodal-signaling mutants (Feldman et al., 1998; Heisenberg and Nusslein-Volhard, 1997; Strahle et al., 1997; Hatta et al., 1991; Feldman et al., 2000; Schier et al., 1997). Morphological defects at 30 hpf included loss of notochord (ranging from discontinuities to complete absence), shortened bodies, bent tail and deficiencies in the prechordal plate leading to ventral forebrain defects such as cyclopia, variable synophthalmia or a unilateral eye (Figs. 3 and S2).

Given that both depletion and overexpression of *zimp7* resulted in axial defects apparently affecting dorsal mesodermal derivatives, we more closely examined these defects. To determine whether the loss and gain of function of Zimp7 produced opposite effects in embryos, we analyzed the expression of axial mesoderm markers in *zimp7*-knockdown and mRNA injected embryos at 30 hpf. WISH experiments demonstrated that *no tail (ntl)* is enhanced and anteriorly expanded in *zimp7* morphants (Figs. 4A, B and S3B), suggesting that this structure might be widened in this situation. In contrast, an increased Zimp7 activity causes loss or disorganization of the notochord, as indicated by a lack of expression of *ntl* (Figs. 4A, C and S3C). Similarly, diminished Zimp7 activity produces embryos with a stronger *sonic hedgehog (shh)* and *colagen2a1a (Col2a1a)* signal in the floor plate, suggesting an expansion of axial markers (Fig. 4D, E G, and H). Measurements of *shh* positive signal in the floor plate confirmed a significant enlargement in the morphants compared to the wild type embryos (Fig. 4D', E' and K). In contrast, hypochordal cells appear normal in the *zimp7* morphants (Fig. 4G and H). Floor plate formation is also defective in *zimp7* overexpressing embryos as indicated by *shh* expression that becomes weaker and interrupted in regions (Fig. 4D and F). These defects are confirmed by the expression of *Col2a1a,* which also shows that embryos with increased *zimp7* expression have a failure in hypochord formation (Fig. 4G and I). *Col2a1a* ectopic signal is found in midline regions indicating that hypochordal or floor plate cells are invading other spaces. In conclusion, these results demonstrate that alterations in Zimp7 levels strongly affect the formation of axial structures. *zimp7* overexpression produces phenotypes indicative of reduced specification of dorsal mesodermal fates, whereas a decrease causes the opposite effect, as evidenced by increases in the expression of axial markers.

Dorsal organizer gene expression is expanded in Zimp7 deficient embryos

Abnormal midline development could be associated with deficient formation of the organizer or abnormalities in dorsal

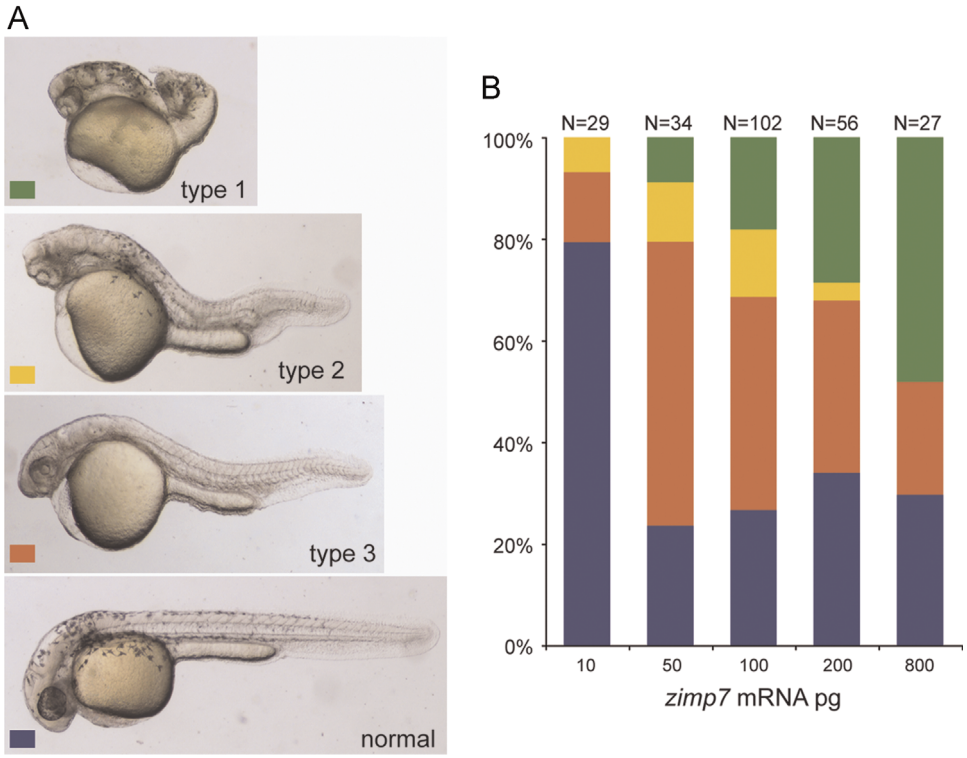

Fig. 3. Zimp7 overexpression produces axial mesoderm defects. Injection of 10–800 pg of *zimp7* mRNA produced malformations that were classified into four categories. (A) Type1 embryos are very severely defective. Type 2 embryos showed cyclopia, anterior truncations, bent tail and shortened body. Type 3 embryos presented a shortened body axis. Lateral views. (B) Distribution of embryonic malformations. Total numbers of embryos are shown at the top. Defects induced by *zimp7* mRNA are dose dependent.

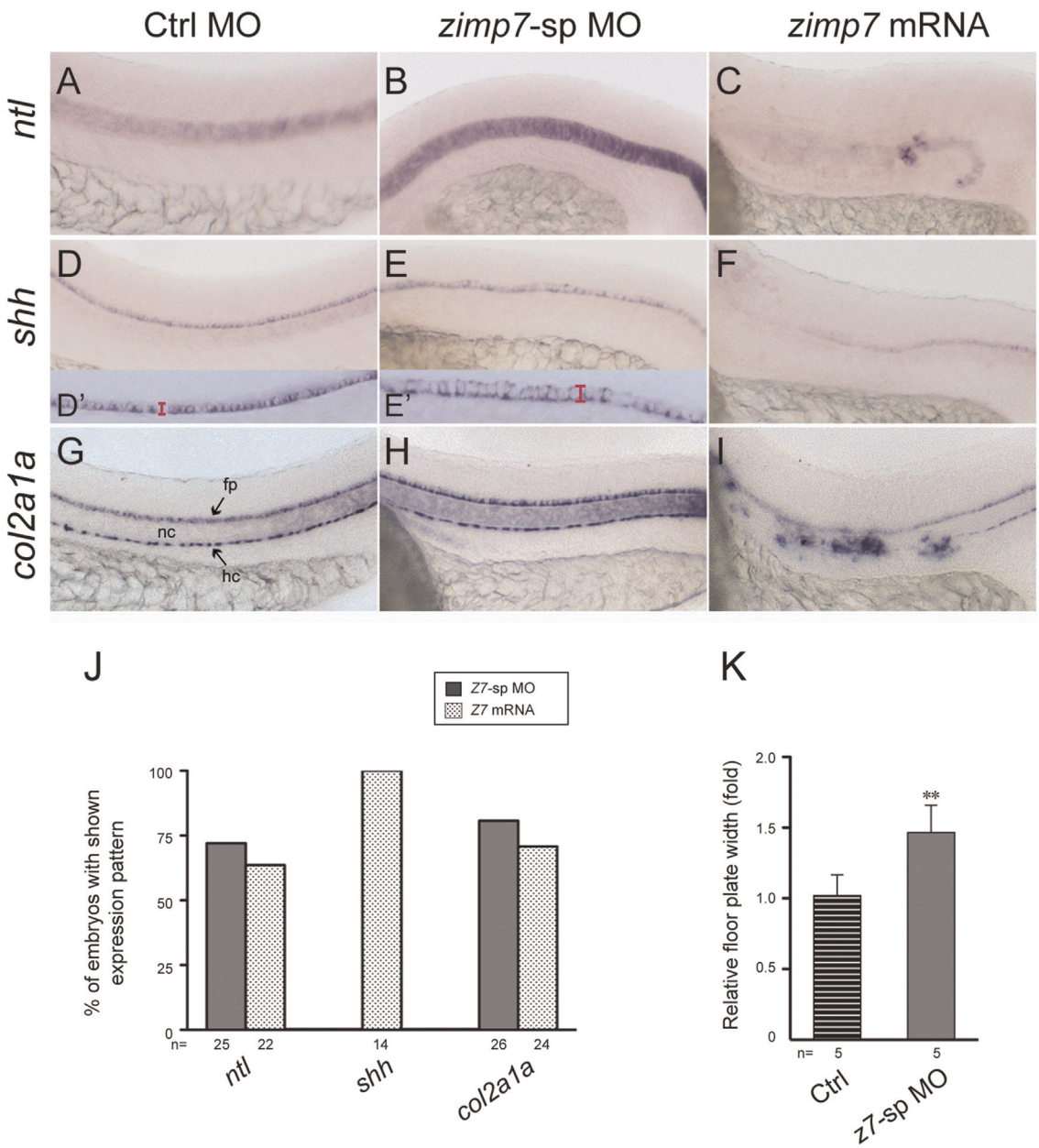

Fig. 4. Loss and gain of function of Zimp7 exert opposite effects in midline structures. Lateral views (anterior is left) of *ntl* (A–C), *shh* (D–F) and *col2a1a* (G–I) expression in Ctrl MO+*p53* MO (A, D, G), *zimp7*-sp MO+*p53* MO (B, E, H) and *zimp7* mRNA (C, F, I) injected embryos at 26 hpf. Compared to the control embryo (A), *ntl* expression in the notochord is increased in a Zimp7 knockdown embryo (B), while it is nearly lost in the gain-of-function embryo (C). Expression of *shh* marks the floor plate. Compared to the control embryo (D) the floor plate is widened in the morphant (E). D' and E' show four-times magnified images of the corresponding embryos, where the engrossment of the floor plate was measured (area indicated with a red bar). *shh* expression reveals the lost of floor plate in embryos injected with a *zimp7* mRNA (F). Expression of *col2a1a* outlines the floor plate and hypochord in a control embryo (G). (H) In knockdown embryos, no significant differences are appreciated in the hypochord, whilst the floor plate exhibits a stronger signal compared to the control embryo. In the embryos overexpressing Zimp7 (I) the signal in the hypochord is defective and ectopic positive signal is detected. fp, floor plate; hc, hypochord; nc, notochord. (J) Percentage of embryos with shown expression pattern in B, C, F and I. Total number of embryos examined indicated at the bottom. (K) Measurements of *shh* positive signal in Ctrl MO and *zimp7*-sp MO injected embryos. $^{**}p < 0.01$.

mesoderm development. To investigate these possibilities, we examined the expression patterns of the dorsal organizer genes *boz* (Fekany et al., 1999), *gsc* (Schultemerker et al., 1994), and *floating head (flh)* (Melby et al., 1997). WISH analysis in *zimp7*-sp MO injected shield stage embryos (6 hpf) showed significantly enlarged expression territories in the *zimp7*-knockdown embryos compared to the control embryos (Fig. 5B, D, G and U). In contrast, at 5 hpf, the mesodermal marker *ntl* was not significantly changed in the morphants (Fig. 5P). Dorsal organizer marker expansion was accompanied by a reduction of expression of the ventral markers *vox* and *vent*, which presented a weaker accumulation of signal at the margin (Fig. 5J, M and V). Occasionally, we noticed that some of the morphants in certain injections of the *zimp7*-sp MO had *vox* and *vent* ectopic domains in the animal ectoderm region (Fig. 5M). Nevertheless, even in embryos with ectopic animal *vox* or *vent* domains, the specific signal in the margin was less extended dorsally (Fig. 5V). In agreement with our findings, the effects of *zimp7* overexpression on *gsc, flh, vox* and *vent* transcription were opposite of the *zimp7* depletion effects: negative regulation of *gsc* and *flh* and upregulation of *vox* and *vent* (Fig. 5E, H, K, N, T–V). On the other hand, *ntl* expression was specifically lost in the presumptive dorsal margin of gain-of-function embryos and remained unaffected in the rest of the margin (Fig. 5Q). *ntl* expression in the dorsal domain is controlled by Nodal signaling, but regulation in the non-axial

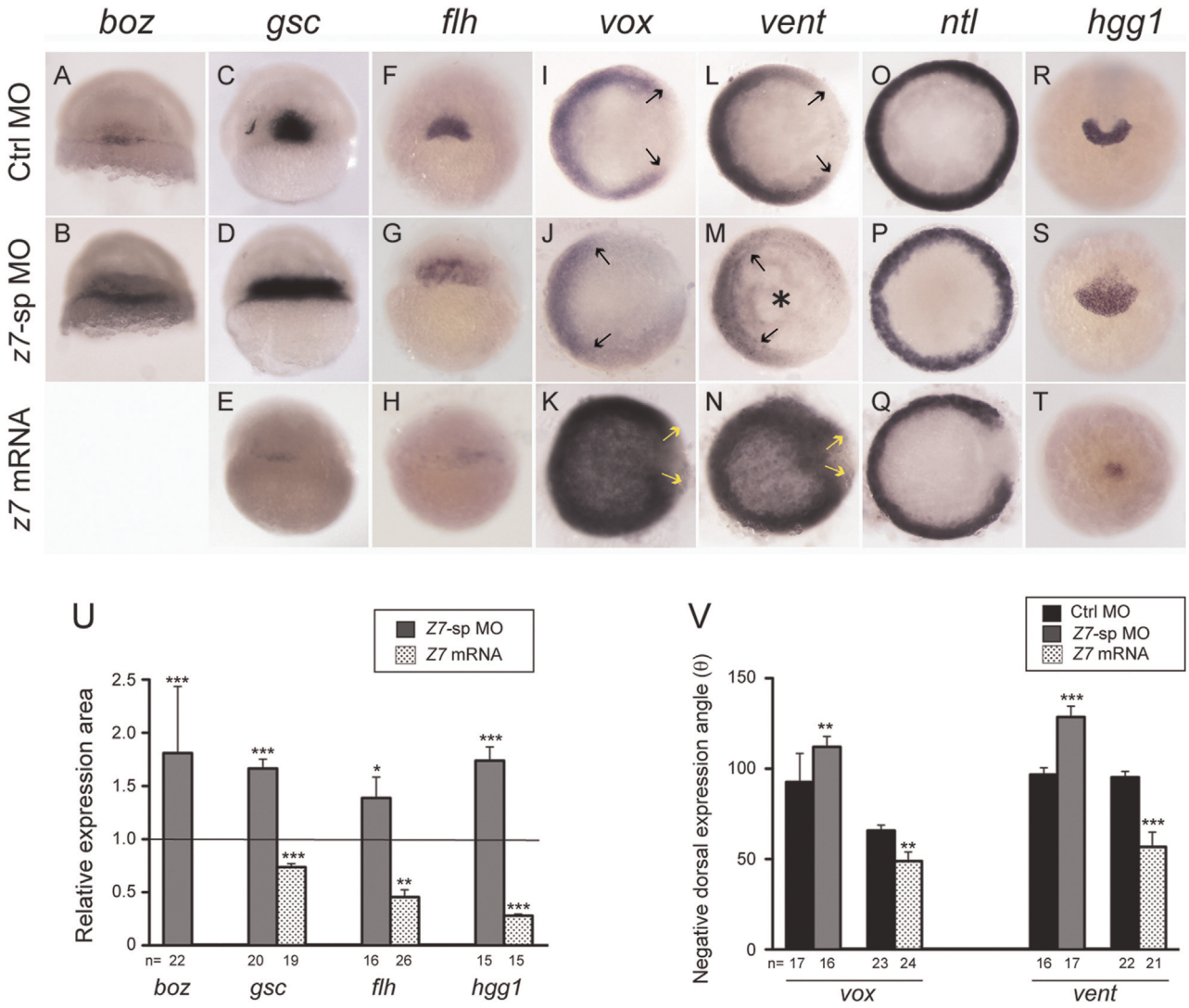

Fig. 5. Zimp7 restricts organizer gene expression. Dorsal and ventral gene expression in embryos at shield (A–N), 5 hpf (O–Q) and 3-somite stage (R–T). Embryos were hybridized to specific marker genes *boz* (A and B), *gsc* (C–E), *flh* (F–H), *vox* (I–K), *vent* (L–N), *ntl* (O–Q) *and hgg1* (R–T). The injected reagents are indicated at the left. *boz*, lateral views, dorsal to the right; *gsc*, and *flh* dorsal views with the animal pole oriented toward the top; *vox*, *vent* and *ntl*, animal pole views with dorsal to the right; *hgg1*, anterior view, dorsal side to the top. Arrows in I–N indicate the angle of marginal expression of ventral genes. An asterisk indicates the ectopic expression of *vent* in the ectoderm. U and V, graphs showing average values obtained from a number of embryos (indicated at the bottom of each bar) as the ones shown in A–T. U, the relative differences in mean expression area in MO and mRNA injected embryos compared to control embryos (horizontal line normalized to one) for the dorsal genes and *hgg1*. V, the average negative expression angle in MO and mRNA injected embryos compared to control embryos for the ventral genes *vox* and *vent*. The number of embryos with given appearance for *ntl* (Q) is 81% ($n=21$). *zimp7* morphants display a significant increase in all dorsal genes as well as in the organizer-induced gene *hgg1* and a reduction in ventral gene expression. Opposite effects are observed when *zimp7* is overexpressed. Notably, besides an increased marginal angle in ventral genes, there is augmented ectodermal expression. $^{*}p < 0.05$; $^{**}p < 0.01$; $^{***}p < 0.001$.

margin is Nodal independent (Harvey et al., 2010). Later stage embryos (shield and 90%-epiboly) confirmed that Zimp7 continues to repress *ntl* during gastrulation and that the repression region corresponds to the dorsal margin (Supplementary Fig. S4A–D). This observation is in line with the *ntl* loss of expression observed in gain-of-function embryos at 30 hpf.

The counteracting effects of Zimp7 loss- and gain-of-function were also evidenced by the dorsal mesoderm marker *hgg1*. During gastrulation, *hgg1* is a specific marker of presumptive hatching gland cells as the *hgg1-positive* cells form the anterior half of the prechordal plate that overlaps with the anterior portion of the *gsc* expression domain (Thisse et al., 1994). In 3-somite stage embryos, the *hgg1* signal was significantly increased in *zimp7* morphants and greatly reduced in *zimp7* overexpressing embryos (Fig. 5S–U). Because specification of the dorsal mesoderm is dependent on Nodal signaling, we tested whether Nodal signaling is induced normally in *zimp7* morphants. We examined expression of the Nodal antagonist *lefty1 (lft1)*. *lft1* is expressed around the margin of the late blastula (Bisgrove et al., 1999). At early gastrula stage (6 hpf), we observed no significant differences in the expression of *lft1* in morphant embryos compared to the control embryos (Supplementary Fig. S4E and F). These data indicate that Nodal signaling in *zimp7* morphants functions normally at an early gastrula stage.

Organizer expansion in *zimp7* morphants is not detected at the blastula period

To explore the participation of Zimp7 within the gene regulatory networks that function throughout mesoderm determination and development, we aimed to distinguish whether Zimp7 acts on the dorsal side as a repressor of dorsal markers or stimulates gene transcription on the ventral side. For this purpose, we quantified and

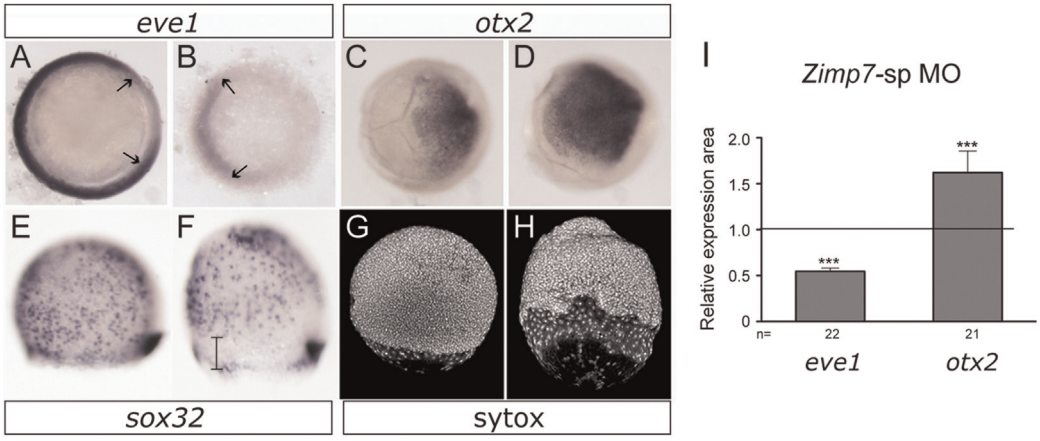

Fig. 6. Analysis of markers at mid-gastrulation. 75% Epiboly stage embryos. (A and B) Decreased Zimp7 activity causes a reduced signal in the ventrolateral mesoderm marker *eve1* (arrows), and up-regulation of the neuroectodermal marker *otx2* (C and D). (E and F) Expression of the endoderm and dorsal forerunner cells (DFCs) marker, *sox32*. Although comparable numbers of endodermal cells are detected in the morphants, the endodermal precursor cells are delayed relative to the DFCs (bar), which remain normal. (G and H) Sytox stained embryos. Similar migration defects are observed, and a bigger gap between the deep layer cells and the enveloping layer cells are observed in the *zimp7* morphants relative to the control. *eve1,* vegetal views, dorsal to the right. *otx2* animal views, dorsal to the right. (E–H) lateral views, animal to the top. (A, C, E, and G) control embryos and (B, D, F, and H) *zimp7* morphants are shown. I, total number of embryos examined (indicated at the bottom) and the mean expression area differences between Ctrl MO and *zimp7*-sp MO injected embryos shown in A–D. The number of embryos with given appearance for *sox32* (F) is 77% ($n=22$) and for Sytox 100% ($n=5$). ***$p < 0.001$.

compared the early zygotic dorsal and ventral marker expression levels in normal and knockdown embryos at the late blastula (4 hpf). Dorsal genes quantified included *boz* and *sqt,* the earliest dorsal targets of maternal β-Catenin signaling, and *gsc*, whose expression is stimulated by *boz* and *sqt*. Because *sqt* is a Nodal ligand, it is also a good marker for early activity of this signaling pathway. The ventral markers we quantified were *vox* and *vent,* whose zygotic expression is initially promoted by the maternal gene *runx2b* and later maintained by Wnt8a and Bmp signaling. Real-time PCR indicated that at the sphere stage, none of these markers changed significantly in the morphants compared to the control embryos (Supplementary Fig. S5C). These results indicate that changes in expression driven by Zimp7 loss- and gain-of-function start later, most likely at gastrulation, and that *boz* and *sqt* transcription is properly initiated by maternal β-Catenin. Therefore, these experiments did not allow us to determine the Zimp7 site of action within the embryo.

A reduction of zimp7 levels results in the loss of non-axial mesoderm and an expansion of neuroectoderm

Because *zimp7* morphants have expanded organizers and excessive axial mesoderm, we examined whether the ventrolateral mesodermal fates were concurrently reduced. An appropriate marker for this analysis is *eve1,* a gene expressed in the ventral mesoderm that regulates the ventrolateral fates of mesodermal progenitor cells and is a good indicator of the non-axial mesoderm status (Joly et al., 1993; Seebald and Szeto, 2011). *eve1* is a transcriptional target of zygotic Wnt8/β-Catenin signaling, similar to *vox* and *vent*; therefore, analysis of *eve1* expression in *zimp7* morphants would also aid in determining whether different Wnt8/β-Catenin signaling targets are affected in these embryos. We found that *eve1* is reduced in *zimp7* morphants both at the onset of gastrulation and at 75% epiboly (Fig. 6A, B and I; and Supplementary Fig. S4G and H). This confirms that dorsal mesoderm expansion occurs at the expense of ventral mesoderm and that different Wnt8a targets are down-regulated in Zimp7 deficient embryos. To assay neuroectodermal patterning in *zimp7* morphants, we examined the expression of *otx2*, a marker of prospective forebrain and midbrain (Mori et al., 1994). Reduction in *zimp7* expression by the *zimp7*-sp MO resulted in a significant expansion of *otx2* expression in late gastrula embryos, indicating increased induction of anterior neuroectoderm (Fig. 6C, D and I). For evaluation of the endoderm, we tested the endodermal marker *casanova/sox32* expression in 75% epiboly embryos (Kikuchi et al., 2001). Although the number of endodermal precursor cells was similar in *zimp7* morphants to that in the control embryos, in the *zimp7*-sp MO injected embryos, these cells were located more animally (Fig. 6E and F), reflecting alterations in cell movements. An irregular or slower migration of the deep layer cells was also observed in embryos with Sytox staining of nuclei (Fig. 6G and H).

Reduction of Zimp7 activity rescues the patterning of ventralized embryos produced by the overexpression of *vox* and *vent*

To directly show the specificity of *zimp7*-sp MO toward the *zimp7* transcript, we carried out rescue experiments. Co-injection of *zimp7*-sp MO with 400–800 pg of zimp7 mRNA markedly restored the expression territories for the *hgg1* and *gsc* genes in morphant embryos compared with the increased levels observed in *zimp7*-sp MO only injected embryos (Fig. 7).

Other rescues were performed to shed further light on the specific participation of Zimp7 within genetic pathways. As we have shown that Zimp7 loss-of-function leads to the up-regulation of dorsal organizer genes, we asked whether the antagonistic interaction that is known to occur between the Vent family homeobox genes and the *gsc* and *boz* organizer genes could be disrupted by the removal of Zimp7. We found that the ventralizing effect produced by the overexpression of *vox* and *vent* in the blastula was compensated by the co-injection of these mRNAs with the *zimp7*-sp MO. Embryos injected with *vox* and *vent* mRNAs presented head or forebrain loss (57%), whereas co-injection with the *zimp7*-sp MO resulted in a significant reduction of these anterior phenotypes (32%) (Fig. 8). To test whether ventralization produced by increasing Bmp activity could also be rescued by a reduction of Zimp7 activity, we co-injected embryos with *zimp7*-sp MO and a previously used translation-blocking MO that targets the secreted Bmp antagonist Chordin (Dal-Pra et al., 2006). Depletion of Chordin caused ventralization in 30 hpf embryos that could not be rescued by the *zimp7*-sp MO (Supplementary Fig. S6C). These results suggest that Zimp7 does not interact with Bmp.

As the axial phenotypes exhibited by 30 hpf embryos with Zimp7 gain-of-function resembled the Nodal signaling mutants, we wanted to determine whether Zimp7 could be acting as a

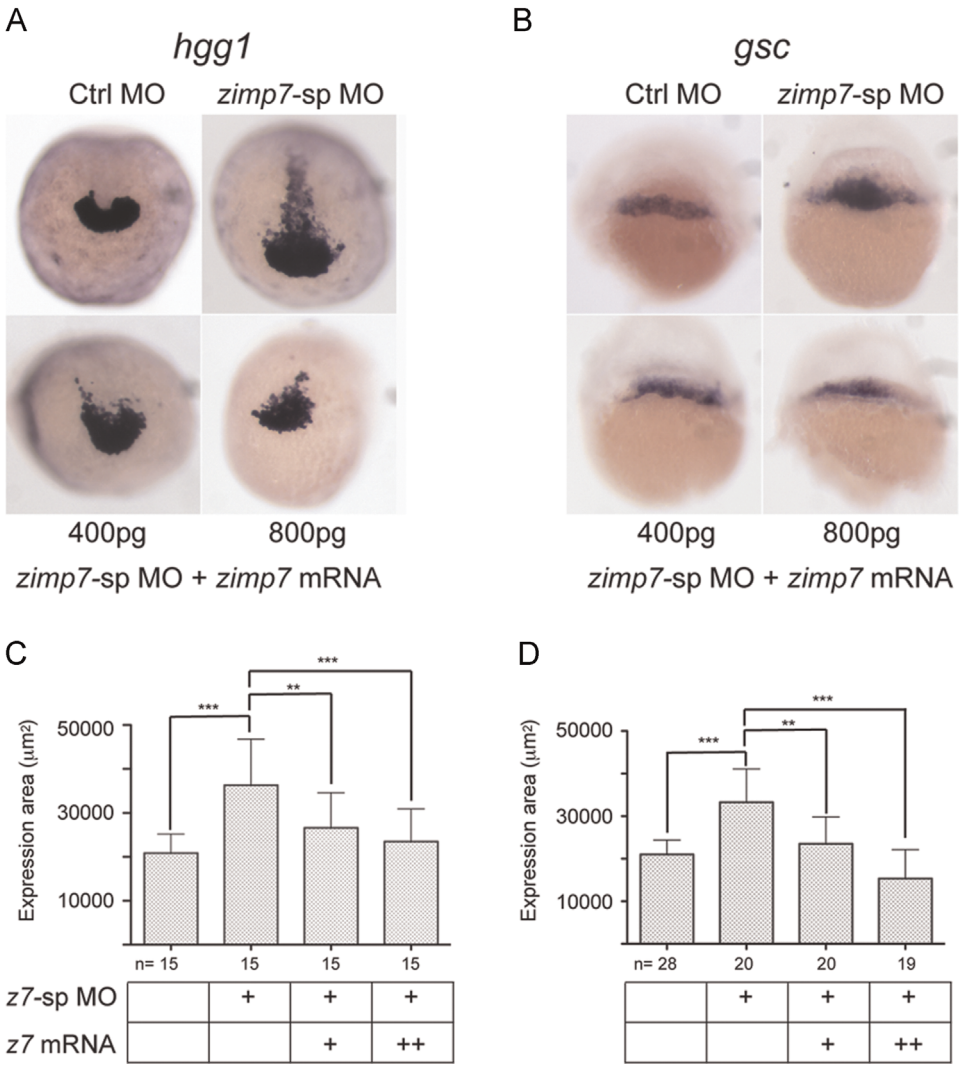

Fig. 7. Co-injection of *zimp7*-sp MO and mRNA restores the normal level of expression of markers in embryos. (A) Anterior views of 3-somite stage embryos with dorsal toward the top. Expression of *hgg1* is shown for control embryos, *zimp7*-sp MO injected embryos and embryos co-injected with *zimp7*-sp MO plus the indicated amounts of *zimp7* mRNA. (B) Expression of *gsc* at shield stage in control embryos, *zimp7*-sp MO injected embryos and embryos co-injected with *zimp7*-sp MO plus the indicated amounts of *zimp7* mRNA. Dorsal views. (C and D) For both markers the expression area was measured for a group of embryos (numbers indicated at the bottom of each bar) and the average area was plotted for each condition. Statistical analysis indicated a significant rescue of the normal level of expression for both markers. Bars represent standard deviation. $^{**}p < 0.01$; $^{***}p < 0.001$.

repressor of this pathway. To test possible interactions between Zimp7 and Nodal signaling, we tried rescue schemes in which the Nodal signaling was increased and others in which the Nodal signaling was limited. To increase Nodal activity, we injected embryos with either *sqt* mRNA, CA*smad2* mRNA that encodes a constitutively active Smad2 (Liu et al., 2013), or a combination of *foxH1* and *eomesodermin* transcripts. Co-injection of *zimp7* mRNA with any of these molecules was unable to rescue the phenotypes observed in the Nodal gain-of-function embryos. Similarly, we used previously reported morpholinos for *oep* or *foxH1* (Pei et al., 2007; Nasevicius and Ekker, 2000) to limit Nodal activity and mRNA encoding a Smad2 dominant negative to test whether we could alleviate the Nodal loss-of-function phenotypes of these embryos by depleting Zimp7 with the *zimp7*-sp MO. None of these assays restored the wild type patterning in the affected embryos (Supplementary Fig. 6A and B). Altogether, these results strongly suggest that Zimp7 does not interact with the Nodal pathway. This notion was further reaffirmed using western blot assays for p-Smad2 in 6 hpf Ctrl MO and *zimp7*-sp MO injected embryos that showed no significant difference in p-Smad2 levels (not shown).

Discussion

In this study, we report the participation of the PIAS-related protein Zimp7 in mesoderm patterning and the modulation of organizer function. We found that *zimp7* morphants have expanded organizers and excessive specification of axial mesoderm and neuroectoderm, concomitant with a loss of non-axial mesoderm fates. Because we obtained embryos with the same apparent morphogenetic defects with two different morpholinos, we believe that their actions are specific. Further confirmation was obtained from rescue experiments and gain-of-function assays. Particularly significant are the reciprocal in situ phenotypes observed in Zimp7 deficient compared to Zimp7 overexpressing embryos, and the demonstration that F0 embryos with CRISPR/Cas-mediated *zimp7* mutations also present similar morphogenetic defects as the ones produced by the MO injections. Notwithstanding, a definitive conclusion will require full genetic analysis of a *zimp7* mutant line.

Although neither the placement of Zimp7 within a genetic pathway nor the determination of its molecular functions were revealed by our data, the evidence we provide allow for the elimination of some signaling pathways and speculation on the

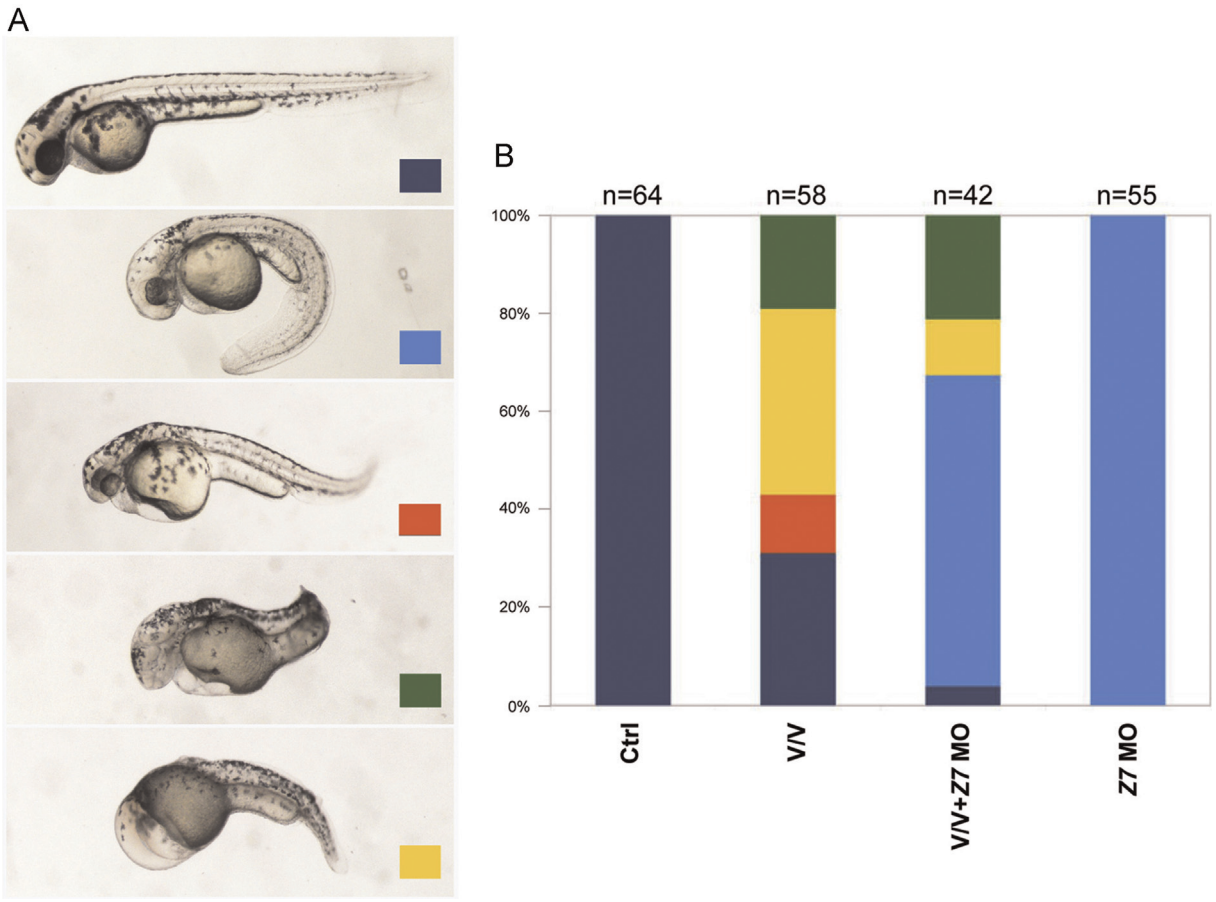

Fig. 8. Reduction of Zimp7 activity suppresses the loss of head detected in Vox and Vent mediated ventralizations. (A) Dark-blue signed embryos are normal looking ones. Injection of 8 ng of the *zimp7*-sp MO+*p53* MO produces embryos with the axial-dorsal phenotype indicated with a light-blue sign. Co-injection of *vox* and *vent* mRNAs produces morphologies displayed and classified in the pictures with orange, green and yellow signs. Orange indicates embryos with mild head defects and a bent tail. Green signed embryos present forebrain loss and shortened axis; yellow signed embryos present a V3-like morphology including the loss of head. (B) A graph showing fractions of embryos at 52 hpf that displayed the indicated phenotypes.

processes in which Zimp7 could be involved. One of these processes is the positive regulation of zygotic Wnt-signaling. Our results suggest that Zimp7 might act as a modulator of this pathway. Among the evidence compatible with that role are the findings that *vox* and *vent* transcription levels are reduced in *zimp7* morphants at the onset of gastrulation, when their regulation is mainly dependent on Wnt activity and that there is a significant reduction in ventrolateral fates, which are controlled by Wnt and Bmp signaling. Even more suggestive is the reduction of Zimp7 activity that partially rescues the ventralized phenotypes produced by simultaneous overexpression of *vox* and *vent* in the blastula. These results are more appealing in light of recent evidence that points to a role for Zimp7 in the regulation of Wnt/β-Catenin signaling pathway activity in mammalian cell lines. The Zimp7-null mouse embryos exhibit decreased expression of CD44, *c-jun* and *Axin2*, three downstream targets of Wnt/β-Catenin.

It is unlikely that Zimp7 is involved in the Bmp signaling pathway. This signaling cascade acts on the ventral side of the embryo to promote ventral cell fates and antagonize dorsal organizer activity. The Bmp cascade shares some downstream targets with the Wnt pathway. However, multiple observations are incompatible with Zimp7 participation in this pathway. One such observation is that *vox*/*vent* gene expression is not yet regulated by Bmp signaling at the onset of gastrulation; another is that we could not rescue the ventralizations induced by Bmp gain-of-function by reducing Zimp7 activity.

The axial phenotype of both Zimp7 loss- and gain-of-function led us to believe that Zimp7 could control dorsal development by antagonizing Nodal activity. For this reason, we performed a variety of experiments designed to demonstrate interactions between Zimp7 and the Nodal pathway. These experiments included different rescue assays and the determination of the status of *Nodal* characteristic markers. However, our results did not support any interaction.

As we were unable to elucidate whether Zimp7 acts on the dorsal or ventral side of the embryo, we cannot exclude the possibility that Zimp7 might be acting as a repressor of organizer genes. In this case, a likely target gene for Zimp7 would be *boz*, which is the earliest organizer gene expressed and is expanded in *zimp7* knockdowns. Zimp7 could be acting as a co-repressor during maternal β-Catenin-mediated *boz* transcription, but at least with the *zimp7*-sp MO, which might start its action on the zygotic *zimp7* transcript before blastula stage, we were unable to detect any changes in *boz* expression at 4 hpf, as revealed by WISH or qPCR experiments (Supplementary Fig. S5). Moreover, so far, Zimp7 has not been reported to be a negative regulator of transcription. Additionally, in zebrafish embryos, *zimp7* transcripts are distributed ubiquitously during development. Because Zimp7 and its homolog Zimp10 have been found to interact with partners involved in a variety of processes, these data suggest that Zimp7 could be involved in the regulation of different pathways of development at the same time. This interpretation would explain some of our observations, such as the presence of ectopic *vox* and *vent* expression domains in the ectoderm of *zimp7* morphants.

Genetic studies in the mouse have shown that inactivating mutations in the Wnt pathway produce severe phenotypes

(Haegel et al., 1995; Grigoryan et al., 2008). Considering the phenotypes shown here for Zimp7 reduction in zebrafish embryos, it is intriguing that mouse *Zimp7* mutants do not present any obvious developmental defects. A possible explanation is that the mouse Wnt pathway might include more redundant modulators than this pathway in the fish. Also it is worth considering that the organizer function appears to differ among the vertebrates. For instance, mice lacking a functional *gsc* gene do not display a gastrulation phenotype or any axial defects (Rivera-Perez et al., 1995; Yamada et al., 1995). It is possible that Zimp7 is essential for molecular aspects that are relevant for specific functions only in some vertebrates during dorsoventral patterning. In conclusion, we demonstrate that in zebrafish Zimp7 has a relevant participation in dorso-ventral patterning.

Acknowledgments

We thank Mary C. Mullins, Arne C. Lekven, David Kimelman, Igor Dawid, Scott Dougan, Steve Harvey, Rebecca Bourdine, Andreas Fritz and Anming Meng for kindly providing plasmids for ISH and mRNA transcription. Lee Kapp for advice in difficult ISH procedures. Ernesto Maldonado for the donation of the fish strain. Dulce Pacheco and Laura Ramírez for assistance with fish maintenance. This work was supported by DGAPA-UNAM, México Grants IN204712, IN202815 and CONACyT, México Grant 236466. R. Moreno-Ayala received the CONACyT, México scholarship 310526.

Appendix A. Supplementary material

Supplementary data associated with this article can be found in the online version at http://dx.doi.org/10.1016/j.ydbio.2015.04.013.

References

Baker, K.D., Ramel, M.C., Lekven, A.C., 2010. A direct role for Wnt8 in ventrolateral mesoderm patterning. Dev. Dyn. 239 (11), 2828–2836. http://dx.doi.org/10.1002/Dvdy.22419.

Bisgrove, B.W., Essner, J.J., Yost, H.J., 1999. Regulation of midline development by antagonism of lefty and nodal signaling. Development 126 (14), 3253–3262.

Dal-Pra, S., Fuerthauer, M., Van-Celst, J., Thisse, B., Thisse, C., 2006. Noggin1 and Follistatin-like2 function redundantly to chordin to antagonize BMP activity. Dev. Biol. 298 (2), 514–526. http://dx.doi.org/10.1016/J.Ydbio.2006.07.002.

Erter, C.E., Wilm, T.P., Basler, N., Wright, C.V.E., Solnica-Krezel, L., 2001. Wnt8 is required in lateral mesendodermal precursors for neural posteriorization in vivo. Development 128 (18), 3571–3583.

Fekany, K., Yamanaka, Y., Leung, T.C., Sirotkin, H.I., Topczewski, J., Gates, M.A., Hibi, M., Renucci, A., Stemple, D., Radbill, A., Schier, A.F., Driever, W., Hirano, T., Talbot, W.S., Solnica-Krezel, L., 1999. The zebrafish bozozok locus encodes Dharma, a homeodomain protein essential for induction of gastrula organizer and dorsoanterior embryonic structures. Development 126 (7), 1427–1438.

Feldman, B., Dougan, S.T., Schier, A.F., Talbot, W.S., 2000. Nodal-related signals establish mesendodermal fate and trunk neural identity in zebrafish. Curr. Biol. 10 (9), 531–534. http://dx.doi.org/10.1016/S0960-9822(00)00469-3.

Feldman, B., Gates, M.A., Egan, E.S., Dougan, S.T., Rennebeck, G., Sirotkin, H.I., Schier, A.F., Talbot, W.S., 1998. Zebrafish organizer development and germ-layer formation require nodal-related signals. Nature 395 (6698), 181–185.

Flores, M.V.C., Lam, E.Y.N., Crosier, K.E., Crosier, P.S., 2008. Osteogenic transcription factor Runx2 is a maternal determinant of dorsoventral patterning in zebrafish. Nat. Cell Biol. 10 (3), 346–U380. http://dx.doi.org/10.1038/Ncb1697.

Gilardelli, C.N., Pozzoli, O., Sordino, P., Matassi, G., Cotelli, F., 2004. Functional and hierarchical interactions among zebrafish vox/vent homeobox genes. Dev. Dyn. 230 (3), 494–508. http://dx.doi.org/10.1002/Dvdy.20073.

Grigoryan, T., Wend, P., Klaus, A., Birchmeier, W., 2008. Deciphering the function of canonical Wnt signals in development and disease: conditional loss- and gain-of-function mutations of alpha-catenin in mice. Genes Dev. 22 (17), 2308–2341. http://dx.doi.org/10.1101/Gad.1686208.

Gutierrez, L., Zurita, M., Kennison, J.A., Vazquez, M., 2003. The Drosophila trithorax group gene tonalli (tna) interacts genetically with the Brahma remodeling complex and encodes an SP-RING finger protein. Development 130 (2), 343–354.

Haegel, H., Larue, L., Ohsugi, M., Fedorov, L., Herrenknecht, K., Kemler, R., 1995. Lack of beta-catenin affects mouse development at gastrulation. Development 121 (11), 3529–3537.

Harvey, S.A., Tumpel, S., Dubrulle, J., Schier, A.F., Smith, J.C., 2010. No tail integrates two modes of mesoderm induction. Development 137 (7), 1127–1135. http://dx.doi.org/10.1242/Dev.046318.

Hatta, K., Kimmel, C.B., Ho, R.K., Walker, C., 1991. The cyclops mutation blocks specification of the floor plate of the zebrafish central-nervous-system. Nature 350 (6316), 339–341. http://dx.doi.org/10.1038/350339a0.

Heisenberg, C.P., Nusslein-Volhard, C., 1997. The function of silberblick in the positioning of the eye anlage in the zebrafish embryo. Dev. Biol. 184 (1), 85–94. http://dx.doi.org/10.1006/dbio.1997.8511.

Hikasa, H., Sokol, S.Y., 2013. Wnt signaling in vertebrate axis specification. Cold Spring Harb. Perspect. Biol. 5 (1), 1–20. http://dx.doi.org/10.1101/cshperspect.a007955.

Huang, C.Y., Beliakoff, J., Li, X., Lee, J., Sharma, M., Lim, B., Sun, Z., 2005. hZimp7, a novel PIAS-like protein, enhances androgen receptor-mediated transcription and interacts with SWI/SNF-like BAF complexes. Mol. Endocrinol. 19 (12), 2915–2929. http://dx.doi.org/10.1210/me.2005-0097.

Hwang, W.Y., Fu, Y.F., Reyon, D., Maeder, M.L., Tsai, S.Q., Sander, J.D., Peterson, R.T., Yeh, J.R.J., Joung, J.K., 2013. Efficient genome editing in zebrafish using a CRISPR-Cas system. Nat. Biotechnol. 31 (3), 227–229. http://dx.doi.org/10.1038/Nbt.2501.

Imai, Y., Gates, M.A., Melby, A.E., Kimelman, D., Schier, A.F., Talbot, W.S., 2001. The homeobox genes vox and vent are redundant repressors of dorsal fates in zebrafish. Development 128 (12), 2407–2420.

Jao, L.E., Wente, S.R., Chen, W.B., 2013. Efficient multiplex biallelic zebrafish genome editing using a CRISPR nuclease system. Proc. Natl. Acad. Sci. USA 110 (34), 13904–13909. http://dx.doi.org/10.1073/Pnas.1308335110.

Jia, S.J., Ren, Z., Li, X., Zheng, Y., Meng, A.M., 2008. Smad2 and smad3 are required for mesendoderm induction by transforming growth factor-beta/Nodal signals in zebrafish. J. Biol. Chem. 283 (4), 2418–2426. http://dx.doi.org/10.1074/Jbc.M707578200.

Joly, J.S., Joly, C., Schultemerker, S., Boulekbache, H., Condamine, H., 1993. The ventral and posterior expression of the zebrafish homeobox gene eve1 is perturbed in dorsalized and mutant embryos. Development 119 (4), 1261–1275.

Kawahara, A., Wilm, T., Solnica-Krezel, L., Dawid, I.B., 2000. Antagonistic role of vega1 and bozozok/dharma homeobox genes in organizer formation. Proc. Natl. Acad. Sci. USA 97 (22), 12121–12126. http://dx.doi.org/10.1073/pnas.97.22.12121.

Kikuchi, Y., Agathon, A., Alexander, J., Thisse, C., Waldron, S., Yelon, D., Thisse, B., Stainier, D.Y.R., 2001. Casanova encodes a novel Sox-related protein necessary and sufficient for early endoderm formation in zebrafish. Genes Dev. 15 (12), 1493–1505. http://dx.doi.org/10.1101/Gad.892301.

Kimmel, C.B., Ballard, W.W., Kimmel, S.R., Ullmann, B., Schilling, T.F., 1995. Stages of embryonic-development of the zebrafish. Dev. Dyn. 203 (3), 253–310.

Krauss, S., Concordet, J.P., Ingham, P.W., 1993. A functionally conserved homology of the Drosophila segment polarity gene-hh is expressed in tissues with polarizing activity in zebrafish embryos. Cell 75 (7), 1431–1444. http://dx.doi.org/10.1016/0092-8674(93)90628-4.

Langdon, Y.G., Mullins, M.C., 2011. Maternal and zygotic control of zebrafish dorsoventral axial patterning. Annu. Rev. Genet. 45, 357–377. http://dx.doi.org/10.1146/annurev-genet-110410-132517.

Lee, J., Beliakoff, J., Sun, Z., 2007. The novel PIAS-like protein hZimp10 is a transcriptional co-activator of the p53 tumor suppressor. Nucleic Acids Res. 35 (13), 4523–4534. http://dx.doi.org/10.1093/Nar/Gkm476.

Lee, S.H., Zhu, C., Peng, Y., Johnson, D.T., Lehmann, L., Sun, Z., 2013. Identification of a novel role of ZMIZ2 protein in regulating the activity of the Wnt/beta-catenin signaling pathway. J. Biol. Chem. 50, 35913–35924. http://dx.doi.org/10.1074/jbc.M113.529727.

Lekven, A.C., Thorpe, C.J., Waxman, J.S., Moon, R.T., 2001. Zebrafish wnt8 encodes two wnt8 proteins on a bicistronic transcript and is required for mesoderm and neurectoderm patterning. Dev. Cell 1 (1), 103–114. http://dx.doi.org/10.1016/S1534-5807 (01)00007-7.

Li, X., Thyssen, G., Beliakoff, J., Sun, Z., 2006. The novel PIAS-like protein hZimp10 enhances Smad transcriptional activity. J. Biol. Chem. 281 (33), 23748–23756. http://dx.doi.org/10.1074/jbc.M508365200.

Li, Y., Allende, M.L., Finkelstein, R., Weinberg, E.S., 1994. Expression of two zebrafish orthodenticle-related genes in the embryonic brain. Mech. Dev. 48 (3), 229–244.

Li, Y.Y., Li, Q., Long, Y., Cui, Z.B., 2011. Lzts2 regulates embryonic cell movements and dorsoventral patterning through interaction with and export of nuclear beta-catenin in zebrafish. J. Biol. Chem. 286 (52), 45116–45130. http://dx.doi.org/10.1074/Jbc.M111.267328.

Liu, X.F., Xiong, C., Jia, S.J., Zhang, Y., Chen, Y.G., Wang, Q., Meng, A.M., 2013. Araf kinase antagonizes Nodal-Smad2 activity in mesendoderm development by directly phosphorylating the Smad2 linker region. Nat. Commun. 4, 1–11. http://dx.doi.org/10.1038/Ncomms2762.

Melby, A.E., Kimelman, D., Kimmel, C.B., 1997. Spatial regulation of floating head expression in the developing notochord. Dev. Dyn. 209 (2), 156–165.

Melby, A.E., Beach, C., Mullins, N., Kimelman, D., 2000. Patterning the early zebrafish by the opposing actions of bozozok and vox/vent. Dev. Biol. 224 (2), 275–285. http://dx.doi.org/10.1006/Dbio.2000.9780.

Miller-Bertoglio, V.E., Fisher, S., Sanchez, A., Mullins, M.C., Halpern, M.E., 1997. Differential regulation of chordin expression domains in mutant zebrafish. Dev. Biol. 192 (2), 537–550. http://dx.doi.org/10.1006/Dbio.1997.8788.

Mori, H., Miyazaki, Y., Morita, T., Nitta, H., Mishina, M., 1994. Different spatio-temporal expressions of three otx homeoprotein transcripts during zebrafish embryogenesis. Brain Res. Mol. Brain Res. 27 (2), 221–231.
Nasevicius, A., Ekker, S.C., 2000. Effective targeted gene 'knockdown' in zebrafish. Nat. Genet. 26 (2), 216–220.
Pei, W.H., Noushmehr, H., Costa, J., Ouspenskaia, M.V., Elkahloun, A.G., Feldman, B., 2007. An early requirement for maternal FoxH1 during zebrafish gastrulation. Dev. Biol. 310 (1), 10–22. http://dx.doi.org/10.1016/J.Ydbio.2007.07.011.
Ramel, M.C., Lekven, A.C., 2004. Repression of the vertebrate organizer by Wnt8 is mediated by Vent and Vox. Development 131 (16), 3991–4000. http://dx.doi.org/10.1242/Dev.01277.
Ramel, M.C., Buckles, G.R., Baker, K.D., Lekven, A.C., 2005. WNT8 and BMP2B co-regulate non-axial mesoderm patterning during zebrafish gastrulation. Dev. Biol. 287 (2), 237–248. http://dx.doi.org/10.1016/J.Ydbio.2005.08.012.
Rivera-Pérez, J.A., Ms., Mallo, Gendron-Maguire, M., Gridley, T., Behringer, R.R., 1995. Goosecoid is not an essential component of the mouse gastrula organizer but is required for craniofacial and rib development. Development 121 (9), 3005–3012.
Ro, H., Dawid, I.B., 2009. Organizer restriction through modulation of Bozozok stability by the E3 ubiquitin ligase Lnx-like. Nat. Cell Biol. 11 (9), 1121–1127 10.1038/ncb1926.
Rodriguez-Magadan, H., Merino, E., Schnabel, D., Ramirez, L., Lonieli, H., 2008. Spatial and temporal expression of Zimp7 and Zimp10 PIAS-like proteins in the developing mouse embryo. Gene Expr. Patterns 8 (3), 206–213. http://dx.doi.org/10.1016/J.Modgep.2007.10.005.
Rytinki, M.M., Kaikkonen, S., Pehkonen, P., Jaaskelainen, T., Palvimo, J.J., 2009. PIAS proteins: pleiotropic interactors associated with SUMO. Cell. Mol. Life Sci. 66 (18), 3029–3041. http://dx.doi.org/10.1007/s00018-009-0061-z.
Sampath, K., Rubinstein, A.L., Cheng, A.H.S., Liang, J.O., Fekany, K., Solnica-Krezel, L., Korzh, V., Halpern, M.E., Wright, C.V.E., 1998. Induction of the zebrafish ventral brain and floorplate requires cyclops/nodal signalling. Nature 395 (6698), 185–189.
Schier, A.F., 2009. Nodal morphogens. Cold Spring Harb. Perspect. Biol. 1 (5), a003459. http://dx.doi.org/10.1101/cshperspect.a003459.
Schier, A.F., Talbot, W.S., 2001. Nodal signaling and the zebrafish organizer. Int. J. Dev. Biol. 45 (1), 289–297.
Schier, A.F., Talbot, W.S., 2005. Molecular genetics of axis formation in zebrafish. Annu. Rev. Genet. 39, 561–613. http://dx.doi.org/10.1146/annurev.genet.37.110801.143752.
Schier, A.F., Neuhauss, S.C., Helde, K.A., Talbot, W.S., Driever, W., 1997. The one-eyed pinhead gene functions in mesoderm and endoderm formation in zebrafish and interacts with no tail. Development 124 (2), 327–342.
Schultemerker, S., Ho, R.K., Herrmann, B.G., Nussleinvolhard, C., 1992. The protein product of the zebrafish homolog of the mouse T-gene is expressed in nuclei of the germ ring and the notochord of the early embryo. Development 116 (4), 1021–1032.
Schultemerker, S., Hammerschmidt, M., Beuchle, D., Cho, K.W., Derobertis, E.M., Nussleinvolhard, C., 1994. Expression of zebrafish goosecoid and no tail gene-products in wild-type and mutant no tail embryos. Development 120 (4), 843–852.
Seebald, J.L., Szeto, D.P., 2011. Zebrafish eve1 regulates the lateral and ventral fates of mesodermal progenitor cells at the onset of gastrulation. Dev. Biol. 349 (1), 78–89. http://dx.doi.org/10.1016/J.Ydbio.2010.10.005.
Sharma, M.J., Li, X.Y., Wang, Y.Z., Zarnegar, M., Huang, C.Y., Palvimo, J.J., Lim, B., Sun, Z.J., 2003. hZimp10 is an androgen receptor co-activator and forms a complex with SUMO-1 at replication foci. EMBO J. 22 (22), 6101–6114.
Shimizu, T., Yamanaka, Y., Nojima, H., Yabe, T., Hibi, M., Hirano, T., 2002. A novel repressor-type homeobox gene, ved, is involved in dharma/bozozok-mediated dorsal organizer formation in zebrafish. Mech. Dev. 118 (1–2), 125–138. http://dx.doi.org/10.1016/S0925-4773(02)00243-5.
Sirotkin, H.I., Dougan, S.T., Schier, A.F., Talbot, W.S., 2000. Bozozok and squint act in parallel to specify dorsal mesoderm and anterior neuroectoderm in zebrafish. Development 127 (12), 2583–2592.
Slagle, C.E., Aoki, T., Burdine, R.D., 2011. Nodal-dependent mesendoderm specification requires the combinatorial activities of FoxH1 and eomesodermin. PLoS Genet. 7 (5), e1002072. http://dx.doi.org/10.1371/Journal.Pgen.1002072.
Solnica-Krezel, L., Driever, W., 2001. The role of the homeodomain protein Bozozok in zebrafish axis formation. Int. J. Dev. Biol. 45 (1), 299–310.
Stachel, S.E., Grunwald, D.J., Myers, P.Z., 1993. Lithium perturbation and goosecoid expression identify a dorsal specification pathway in the pregastrula zebrafish. Development 117 (4), 1261–1274.
Strahle, U., Jesuthasan, S., Blader, P., Garcia-Villalba, P., Hatta, K., Ingham, P.W., 1997. One-eyed pinhead is required for development of the ventral midline of the zebrafish (*Danio rerio*) neural tube. Genes Funct. 1 (2), 131–148.
Talbot, W.S., Trevarrow, B., Halpern, M.E., Melby, A.E., Farr, G., Postlethwait, J.H., Jowett, T., Kimmel, C.B., Kimelman, D., 1995. A homeobox gene essential for zebrafish notochord development. Nature 378 (6553), 150–157. http://dx.doi.org/10.1038/378150a0.
Thisse, B., Pflumio, S., Fürthauer, M., Loppin, B., Heyer, V., Degrave, A., Woehl, R., Lux, A., Steffan, T., Charbonnier, X., 2001. Expression of the zebrafish genome during embryogenesis. ZFIN Direct Data Submiss.
Thisse, C., Thisse, B., 2008. High-resolution in situ hybridization to whole-mount zebrafish embryos. Nat. Protoc. 3 (1), 59–69. http://dx.doi.org/10.1038/Nprot.2007.514.
Thisse, C., Thisse, B., Halpern, M.E., Postlethwait, J.H., 1994. Goosecoid expression in neurectoderm and mesendoderm is disrupted in zebrafish cyclops gastrulas. Dev. Biol. 164 (2), 420–429. http://dx.doi.org/10.1006/Dbio.1994.1212.
Toyama, R., O'Connell, M.L., Wright, C.V., Kuehn, M.R., Dawid, I.B., 1995. Nodal induces ectopic goosecoid and lim1 expression and axis duplication in zebrafish. Development 121 (2), 383–391.
Westerfield, M., 2000. The Zebrafish Book: A Guide for the Laboratory Use of Zebrafish (*Danio rerio*). University of Oregon Press, Eugene, OR.
Yamada, G., Mansouri, A., Torres, M., Stuart, E.T., Blum, M., Schultz, M., Derobertis, E. M., Gruss, P., 1995. Targeted mutation of the murine goosecoid gene results in craniofacial defects and neonatal death. Development 121 (9), 2917–2922.
Yan, Y.L., Hatta, K., Riggleman, B., Postlethwait, J.H., 1995. Expression of a type-II collagen gene in the zebrafish embryonic axis. Dev. Dyn. 203 (3), 363–376.